THE ASTROPHYSICAL JOURNAL, 369: L59–L61, 1991 March 10


# FIRST RESULTS FROM THE FAINT OBJECT CAMERA: IMAGES OF THE GRAVITATIONAL LENS SYSTEM G2237+0305[1]

P. CRANE,[2,3] R. ALBRECHT,[2,4,5] C. BARBIERI,[2,6] J. C. BLADES,[2,7] A. BOKSENBERG,[2,8] J. M. DEHARVENG,[2,9] M. J. DISNEY,[2,10] P. JAKOBSEN,[2,11] T. M. KAMPERMAN,[2,12] I. R. KING,[2,13] F. MACCHETTO,[2,5,7] C. D. MACKAY,[2,14] F. PARESCE,[2,5,7] G. WEIGELT,[2,15] D. BAXTER,[7] P. GREENFIELD,[7] R. JEDRZEJEWSKI,[7] A. NOTA,[6,7] AND W. B. SPARKS[7]

*Received 1990 October 15; accepted 1990 November 27*

## ABSTRACT

Images of the gravitational lens system G2237+0305 have been obtained with the Faint Object Camera on board the *Hubble Space Telescope*. A preliminary analysis of these images is reported here and includes measurements of the relative positions and magnitudes of the lensed images of the QSO, and of the lensing galaxy. No evidence is found for a fifth lensed image.

*Subject headings:* galaxies: general — gravitational lenses — quasars

## 1. INTRODUCTION

The gravitational lens G2237+0305, discovered by Huchra et al. (1985), appears as a result of an extremely fortuitous alignment of a background QSO at $z = 1.695$ with the nucleus of a 14th mag foreground galaxy at $z = 0.039$. This lens produces four distinct QSO images (see Yee 1988 and Irwin et al. 1989 for the best ground-based images) arranged in a roughly symmetrical cross centered on the nucleus of the galaxy. Models of this lens presented by Schneider et al. (1988) and Kent & Falco (1988) imply the alignment is better than 0″.1. The a posteriori estimates of the probability of such a close alignment of a galaxy and a QSO of sufficient luminosity occurring anywhere in our sky range from $10^{-2}$ to $10^{-5}$, depending on the model. If such estimates are correct, this lens is almost certainly unique. Because of the unusual proximity of the lensing galaxy, the number of images produced, the relatively small time delay between images, and the likelihood of microlensing events, this system makes a favorable candidate for trying to determine (1) the $M/L$ ratio of the galaxy's central region, (2) the size of the continuum emission region in the QSO (Kayser, Refsdal, & Stabell 1986), (3) the interstellar absorption law in an external galaxy (Yee 1988), and (4) the value of $H_0$ (Refsdal 1964) and $\Lambda_0$ (Paczyński & Gorski 1981; Gott 1987).

Although ground-based images of this lens with excellent seeing (about 0″.6 FWHM) have resolved the four QSO images, clearly better resolution is required to (1) improve or confirm their positions and magnitudes, (2) better determine the galaxy's nuclear structure which has an important effect on the QSO images, and (3) search for the fifth image predicted near the nucleus by current lensing theory.

*Hubble Space Telescope* (*HST*) observations with the Faint Object Camera (FOC) were expected to improve our knowledge in these areas. With the serious spherical aberration present in the *HST* primary mirror, the point-spread function (PSF) now has the light distributed in a 2″ radius halo while retaining only 15% of the light within a 0″.1 radius (see Burrows 1991). Nevertheless, the PSF still has a relatively sharp core (FWHM ≈ 0″.06) which should yield high-resolution information. For this reason G2237+0305 was chosen as part of a series of observations made to assess the range and quality of data that could be obtained in spite of the degraded performance of the *HST* optics. This *Letter* reports preliminary results of our first exposures of this gravitational lens. Because of the present state of calibration of the telescope and FOC, it was possible to perform only limited data analysis on the images. Subsequent papers will present more detailed analyses based on these and future exposures taken with the FOC.

## 2. OBSERVATIONS

The FOC consists of two independent optical relays with effective focal ratios of f/48 and f/96. Each optical relay is equipped with a photon-counting detector capable of producing images through various filters and prisms. The Faint Object Camera Handbook (Paresce 1990) describes in detail the optical and imaging modes available, as well as the filters and performance characteristics of the FOC.

Two images of the galaxy-QSO system were obtained with the f/96 optical train of the FOC on 1990 August 27. The first was a 597 s acquisition exposure and was taken using the F430W and F2ND (2 mag neutral density) filters; it is slightly trailed and underexposed. This image has a size of 512 × 1024

[1] Based on observations with the NASA/ESA *Hubble Space Telescope*, obtained at the Space Telescope Science Institute, which is operated by AURA, Inc., under NASA contract NAS 5-26555.

[2] Member FOC Investigation Definition Team.
[3] European Southern Observatory, Karl Schwarzschild Strasse 2, D-8046
[4] Space Telescope European Coordinating Facility, Karl Schwarzschild Strasse 2, D-8046 Garching, Germany.
[5] Astrophysics Division, Space Science Department of ESA.
[6] Osservatorio Astronomico di Padova, Vicolo Osservatorio, 5, I-35122 Padova, Italy.
[7] Space Telescope Science Institute, 3700 San Martin Drive, Baltimore, MD 21218.
[8] Royal Greenwich Observatory, Madingley Road, Cambridge CB3 0EZ, UK.
[9] Laboratoire d'Astronomie Spatiale du CNRS, Traverse du Siphon, Les Trois Lucs, F-13012 Marseille, France.
[10] Department of Physics, University College of Cardiff, P.O. Box 713, Cardiff CF1 3TH, Wales, UK.
[11] Astrophysics Division, Space Science Department of ESA, ESTEC, NL-2200 AG Noordwijk, The Netherlands.
[12] Laboratory for Space Research, Space Research Institute, Sorbonnelaan 2, NL-3584 CA, Utrecht, The Netherlands.
[13] Astronomy Department, University of California, Berkeley, CA 94720.
[14] Institute of Astronomy, Madingley Road, Cambridge CB3 0HA, UK.
[15] Max-Planck-Institut für Radioastronomie, Auf dem Hügel 69, D-5300 Bonn 1, Germany.

pixels where the pixels are rectangular and have a size of approximately 0".044 × 0".022 resulting in a field size of 22" × 22". The second image, shown in Figure 1 (Plate L18), is a 1496 s exposure taken through the F502M filter and intended to show the galaxy and the QSO images. This image has a size of 512 × 512 pixels where the pixels are square and have an approximate size of 0".022 × 0".022 resulting in a field size of 11" × 11". This exposure was taken with the telescope in coarse track mode (as opposed to fine lock); as a consequence there is extra jitter in the pointing and some resulting reduction in the resolution. The F430W filter is close to a Johnson $B$ filter and the F502M approximates a Gunn $g$ filter.

Both images were flat-fielded and the geometric distortion corrected using algorithms developed by the FOC team. The reseau marks (which are fiducial references on the photocathode) were not removed and are evident. Figure 1 shows the four lensed images of the QSO. Between these images we see a diffuse source which we take to be the nucleus of the lensing galaxy. The brightest of the lensed images, B, has a peak count of 430 counts, and the corresponding count rate is well within the FOC linear range for point sources (Paresce 1990). The "galaxy" has approximately 45 counts pixel$^{-1}$ at maximum.

## 3. ANALYSIS

Since the wings of the PSFs at the four QSO image positions overlap each other and the position of the galaxy nucleus, our initial inclination was to attempt some image deconvolution. This approach considerably improved the cosmetic appearance of the four QSO components, but the signal from the galaxy center, being of very low signal-to-noise ratio, was severely degraded. We therefore decided to confine our analysis procedures to the unprocessed image, since we can account for the effects of the PSF wings sufficiently well to derive measurements of fluxes and positions to good accuracy and retain a thorough understanding of the sources of errors.

The relative brightnesses of the individual QSO images were determined using the IRAF "imexamine" routine. This is a simple aperture photometry routine that calculates the total flux from the pixels interior to a circular aperture, while subtracting a background determined from an annulus around the aperture. An aperture radius of 5 pixels was chosen, which is known to contain approximately 20% of the flux from a point source, and the background was calculated as the median of the pixels that lie between 6 and 8 pixels from the center of the point source as calculated by the routine using a simple centroid. Although this procedure accounts for only a fraction of the light from each image, it is the same fraction in each case and is therefore a reasonably good measure of the relative intensity. The background is made up from the wings of the point source being measured, the wings of the other QSO components, the galaxy and detector background, and since the background was determined in the same way for each of the QSO components, the relative brightnesses derived should be an accurate measurement of the true relative magnitudes.

The uncertainty originates mainly from the background evaluation and the fine-scale flat-field response (which is not corrected in the flat-fielding process) and is estimated to be about 0.05 mag for the brightest two components, and about 0.1 mag for the faintest two, where the background uncertainties are proportionately higher. The relative magnitudes are listed in the first two columns of Table 1 and are compared to previous observations (when several measurements were available at a given time period, we have retained for comparison the measurements through the filter most comparable to that used in our observations). There is clear evidence that the B QSO image is roughly 0.15 mag brighter than the A QSO image, confirming the claim of Pettersen (1990) for observations taken in the same time period. This is also fully consistent with the fading of the A component (Corrigan et al. 1990) following the microlensing event reported in Irwin et al. (1989).

TABLE 1

RELATIVE MAGNITUDES

| Object | $\Delta g$[a] | $\Delta B$[a] | $\Delta r$[b] | $\Delta R$[c] | $\Delta g$[d] | $\Delta r$[e] |
|---|---|---|---|---|---|---|
| A ......... | 0.14 | 0.14 | 0.15 | −0.53 | −0.21 | 0.10 |
| B ......... | 0.00 | 0.00 | 0.00 | 0.00 | 0.00 | 0.00 |
| C ......... | 0.81 | 0.84 | ... | 0.61 | 0.48 | 0.43 |
| D ......... | 1.02 | 1.16 | ... | 0.84 | 0.71 | 0.93 |

[a] This *Letter*. The relative magnitudes have an error of ±0.05 for component A and ±0.10 for components C and D. An estimate of the $g$ and $B$ magnitudes of the B component is 17.60 ± 0.10 and 17.82 ± 0.07, respectively. Data from 1990 Aug 27.

[b] Pettersen 1990. Data 1990 Aug 25–31.

[c] Irwin et al. 1989. Data from 1988 Aug 18.

[d] Yee 1988. Data from 1987 Sep 25.

[e] Schneider et al. 1988. Data from 1985 Oct 13.

To compare the absolute photometry with ground-based measurements of the QSO components, the photometric zero points were determined using FOC observations of the UV spectrophotometric standard star BPM 16274 (Turnshek et al. 1990). Simple "box" photometry of this star and the B lensed component gives $B_{\rm B} = 17.82 \pm 0.07$. Determining the zero point for the $g$ magnitude is less straightforward. Although the F502M filter approximates a $g$ filter, and the most similar ground-based measurements are also through a $g$ filter, the standard star has only $B$ and $V$ photometry published. Using the relation from Kent (1985) $g = V - 0.19 + 0.41(B-V)$ to find the expected $g$ magnitude of the standard star, and again using "box" photometry, gives $g_{\rm B} = 17.60 \pm 0.10$. These zero-point determinations are uncertain due to a lack of knowledge of the color equations for the FOC filters, as well as due to imperfect knowledge of the background contributions at the position of the B QSO component. Further calibration observations will provide knowledge of the color equations. We assign an error of 0.1 to the magnitude to account for our estimated error. Nevertheless, comparison with the magnitudes in Yee (1988) shows that the brightness of A is similar to that measured in 1987, while the B component is 0.4 mag brighter now.

The relative positions of the four images of the QSO and of the center of the "galaxy" have been measured using a simple centroiding algorithm. The uncertainty in the position of the individual images was typically 0.1 pixels. Table 2 lists the results obtained for the positions of the four QSO images and for the "galaxy." The columns labeled $\Delta X$ and $\Delta Y$ are the

TABLE 2

RELATIVE POSITIONS

| Object | $\Delta X$ | $\Delta Y$ | ΔE | ΔN |
|---|---|---|---|---|
| A .............. | 0".000 | 0".000 | 0".000 | 0".000 |
| B .............. | 0.108 | 1.796 | −0.672 | 1.673 |
| C .............. | −0.976 | 0.941 | 0.626 | 1.202 |
| D .............. | 0.646 | 0.761 | −0.854 | 0.517 |
| Galaxy ......... | −0.209 | 0.917 | −0.093 | 0.936 |

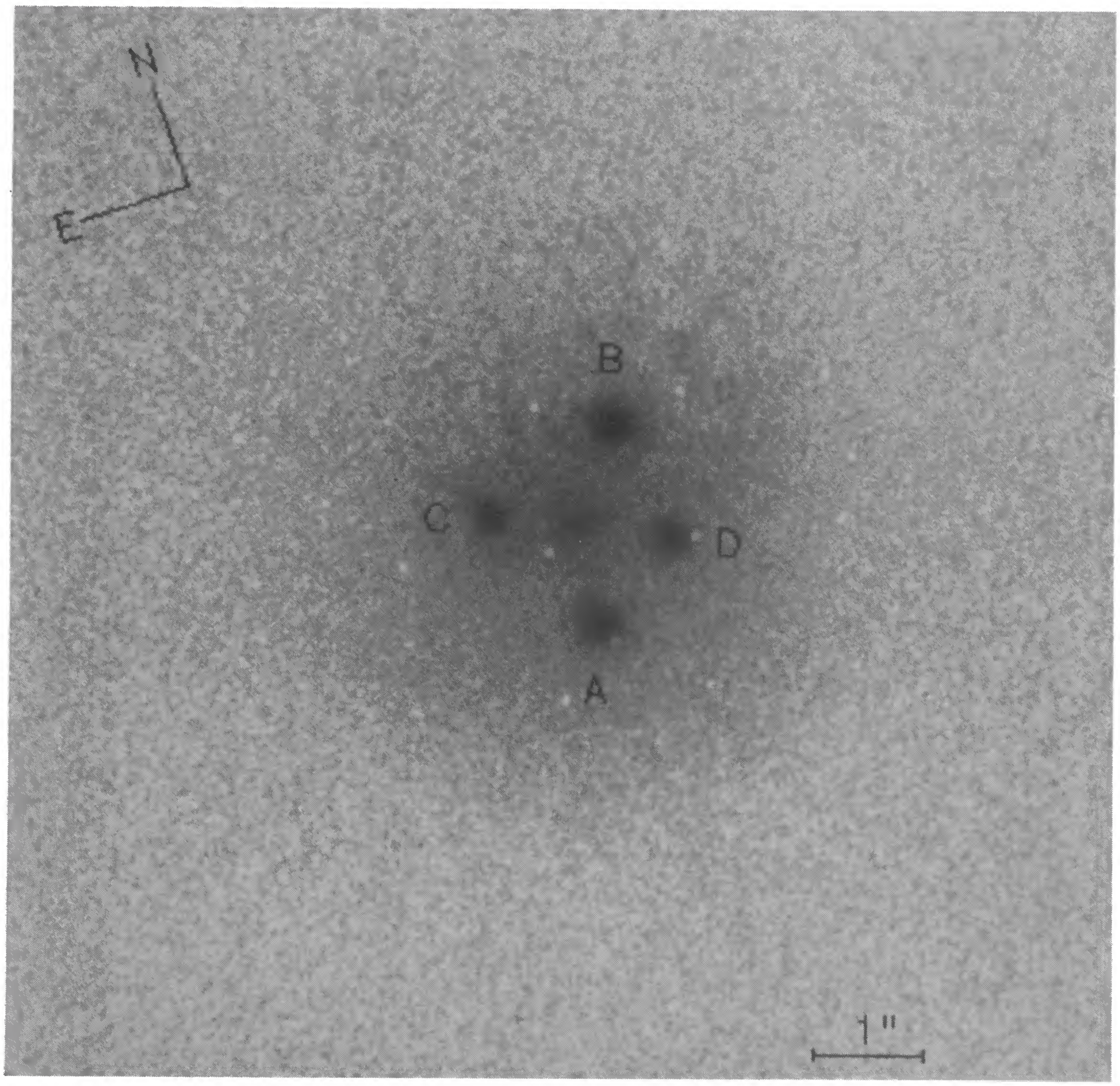


FIG. 1.—Faint Object Camera image of the gravitational lens system G2237+0305, taken with the F502M filter, which approximates a *g* filter. The four lensed images of the QSO are clearly seen, and the center of the galaxy is also evident. The reseau marks on the FOC detector are also visible. Following the nomenclature of several other authors, the lensed images are referred to as A, B, C, and D as indicated. A logarithmic intensity scale has been used.

CRANE et al. (see 369, L60)

relative positions in line and frame directions converted to arcseconds. The columns labeled ΔE and ΔN are the results of rotating by 18°.47 to give the relative coordinates along the directions east and north. The rotation angle is derived from the spacecraft roll angle.

Our relative positions, which presently have a formal error of only ±0″.005 (largely due to limitations in the correction for detector distortion), are consistent with the earlier ground-based measurements of Yee (1988) and of Irwin et al. (1989) whose quoted errors, between 0″.01 and 0″.02, are, however, dependent on fairly intricate modeling procedures.

Although the central region of the "galaxy" appears to have a bright nucleus which increases in brightness all the way to the center, it does not exhibit the same tight core as the QSO images (see Fig. 1). The "galaxy" core is considerably broader (FWHM ∼ 0″.4) than the typical QSO image (FWHM ∼ 0″.08). To examine it more carefully, we have subtracted from the $g$ frame four point spread functions at the positions of A, B, C, and D, scaled in intensity according to Table 1. Figure 2 shows a contour plot of the residual image obtained from this subtraction.

As mentioned earlier, this image of G2237+0305 was obtained with *HST* in coarse track, the effect of which is to broaden the cores of the QSO images so that they have FWHM ∼ 0″.08 (compared to 0″.06 for the stellar PSF which was obtained in fine lock). Because of this we find that, although the scaling of the four PSFs is considered reliable (to about 1%–2%), the subtraction leaves visible residuals within about 8 pixels of the positions of the QSO components.

In the F502M ($g$) frame, at the position of the "galaxy" nucleus, the overlapping PSFs are estimated to contribute about 8 counts in the raw image (about 20%). The subtracted frame shows a peak value of about 35 counts pixel$^{-1}$ and has a profile which falls off relatively smoothly all the way to the edge of the frame. It should also be borne in mind that the PSF, with 80% of the light outside of the sharp core, is extremely dispersive, and therefore more specific comments regarding the intrinsic profile of the extended object would be unwise at this stage.

The positions of this diffuse image, given in Table 2 and labeled "galaxy," coincide with the centroid of the galaxy given by Yee (1988) to within 0″.014. Its $B - g$ color is approximately 1 mag redder than that of the B component. From its shape, position, and color, it is presumed to be the core of the lensing galaxy. More photons and a clear understanding of the effect of the PSF will be needed to deconvolve the parameters such as ellipticity and position angle needed for precise lensing models.

Lensing theory (e.g., Blandford & Kochanek 1987) always predicts that extended, transparent gravitational lenses should produce an odd number of lensed images. However, there is no evidence for a fifth image in these data. In order to obtain a quantitative limit, we have used artificial stellar images created with the task "addstar" in the photometric package

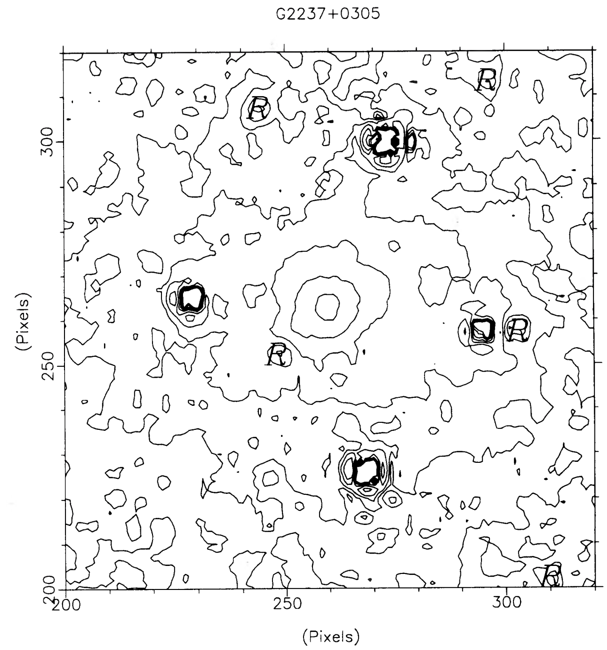


FIG. 2.—Contour map (2″.9 × 2″.9) of the central regions of the $g$ frame after subtraction of the QSO components and smoothing. The reasons for the residuals at the QSO positions are given in the text. The central object is clearly diffuse (FWHM ∼0″.4). We find no evidence for a fifth lensed image. The highest contour in the central image is at 28.3 counts pixel$^{-1}$ with subsequent contours at 19.4, 13.3, 9.0, and 6.2. Note: the positions of the fiducial reference marks (reseaux) have been indicated with the symbol R.

DAOPHOT. We have found that a fifth image 30 times fainter than image B would have been detected over the general background between the four QSO lensed images. Within a radius of about 0″.15 from the nucleus of the galaxy, which corresponds roughly to the second innermost contour in Figure 2, this limit is weaker by a factor of 2. At the very center, as discussed earlier, the red color measured is an evidence that we are seeing the core of the galaxy and not the fifth image. A better limit would be set by a complete model of the system used to predict the expected position of the fifth image.

The Faint Object Camera is the result of many years of hard work and important contributions by a number of highly dedicated individuals. In particular, we wish to thank ESA *HST* Project Manager Robin Laurance, the ESA/*HST* Project Team and the European contractors for building an outstanding scientific instrument. The FOC IDT Support Team, D. Baxter, P. Greenfield, R. Jedrzejewski, and W. B. Sparks, acknowledge support from ESA through contract 6500/85/NL/SK. P. Crane and I. R. King acknowledge support from NASA through contracts NAS5-27760 and NAS5-28086.

## REFERENCES

Blandford, R. D., & Kochanek, C. S. 1987, ApJ, 321, 658
Burrows, C., et al. 1990, ApJ, 369, L21
Corrigan, R. T., Irwin, M. J., Hewett, P. C., & Webster, R. L. 1990, in Gravitational Lensing, ed. Y. Mellier, B. Fort, & G. Soucail (Berlin: Springer), 206
Gott, J. R. 1987, in IAU Symposium 117, Dark Matter in the Universe, ed. J. Kormendy & G. R. Knapp (Dordrecht: Reidel), 219
Huchra, J., Gorenstein, M., Kent, S., Shapiro, I., Smith, G., Horine, E., & Perley, R. 1985, AJ, 90, 691
Irwin, M. J., Webster, R. L., Hewett, P. C., Corrigan, R. T., & Jedrzejewski, R. I. 1989, AJ, 98, 1989
Kayser, R., Refsdal, S., & Stabell, R. 1986, A&A, 166, 36
Kent, S. M. 1985, PASP, 97, 165
Kent, S. M., & Falco, E. E. 1988, ApJ, 96, 1570
Paczyński, B., & Gorski, K. 1981, ApJ, 248, L101
Paresce, F. 1990, The Faint Object Camera Handbook (Baltimore: Space Telescope Science Institute)
Pettersen, B. R. 1990, IAU Circ., No. 5099
Refsdal, S. 1964, MNRAS, 128, 307
Schneider, D. P., Turner, E. L., Gunn, J. E., Hewitt, J. N., Schmidt, M., & Lawrence, C. R. 1988, AJ, 95, 1619
Turnshek, D. A., Bohlin, R. C., Williamson, R. L., Lupie, O., & Koornneef, J. 1990, AJ, 99, 1243
Yee, H. K. C. 1988, AJ, 95, 1331